Determination of Angular Separation Between Spacecraft and Quasars with the Very Long Baseline Array

G. Lanyi,[1] J. Border,[1] J. Benson,[2] V. Dhawan,[2] E. Fomalont,[3] T. Martin-Mur,[4]
T. McElrath,[4] J. Romney,[2] and C. Walker[2]

The interferometric technique of phase referencing was used to determine the relative angular positions of the Mars Exploration Rover B (MER-B) spacecraft with respect to angularly nearby quasars. The final cruise state of MER-B was observed in three sessions by the Very Long Baseline Array (VLBA) as part of a larger feasibility study to determine the accuracy of this technique. This article summarizes the VLBA observations and reductions of the nominal 10-station (45-baseline) observables, the incorporation of the delay data within the Orbit Determination Program, and the comparison of the VLBA and the Deep Space Network (DSN)-based delta differential one-way ranging (ΔDOR) results. The pathway from VLBA observations to navigation use of the data is well-defined. The analysis shows that the formal accuracy of the VLBA-determined approximately declination-projected position of the spacecraft is 1.2 nanoradians (nrad) when the correlation among different-station delay observables is ignored. This formal accuracy, deduced from observed residual delay scatter, is about two times smaller than the corresponding result from the DSN ΔDOR observations. While the effect of quasar position and station location errors was included as a priori error in the estimate of formal errors, note that, to highlight the impact of improved measurement precision, the formal *accuracy values do not include the larger Mars ephemeris and planetary-to-inertial-frame tie and the effects of possible modeling errors. These contributions, as well as those from tropospheric refraction errors and the assumed 0.7-nrad uncertainty of the particular quasar position, must be reduced in order to obtain more accurate positions in the future.*

---

[1] Tracking Systems and Applications Section.

[2] National Radio Astronomy Observatory, Socorro, New Mexico.

[3] National Radio Astronomy Observatory, Charlottesville, Virginia.

[4] Flight Dynamics Section.

The research described in this publication was carried out by the Jet Propulsion Laboratory, California Institute of Technology, and the National Radio Astronomy Observatory, under National Aeronautics and Space Administration contract and grant. The National Radio Astronomy Observatory is a facility of the National Science Foundation operated under cooperative agreement by Associated Universities, Inc.

I. Introduction

The angular spacecraft position determination technique delta differential one-way ranging (ΔDOR) has been in existence over two decades [1]. The position of the spacecraft is determined relative to the predetermined reference frame of quasars by measuring the group delays on two intercontinental Deep Space Network (DSN) baselines. For the quasar, the group delay is obtained from its wideband noise-like emission. For the spacecraft, a pair of tones, with currently less than 100-MHz separation, can be turned on, and these are used to determine the group delay to the spacecraft. The ΔDOR technique was successfully used for Mars Exploration Rover (MER) tracking, obtaining an Orbit Determination Program (ODP) estimate of formal accuracy of 2.4 nanoradians (nrad) for the declination-projected position of the spacecraft based on a 5-day data span.

Accurate differential angular positions between quasars can also be obtained from source images based on differential interferometric phase, a technique that is referred to as very long baseline interferometry (VLBI) phase referencing [2]. Recent Very Long Baseline Array (VLBA) results show that relative quasar positions with accuracy $<$0.25 nrad are possible. Differential angular position measurements among spacecraft and between quasars and spacecraft are also possible using either the VLBI group-delay or phase-referencing technique. The U.S. radio astronomy network has been utilized for deep-space tracking of the Pioneer-13 Venus probes in a spacecraft-to-spacecraft differential VLBI mode. Another relevant U.S. antenna network for spacecraft navigation could be the VLBA. Besides the possible increase in positional accuracy, the VLBA could track the spacecraft without the dedicated tones and with the benefit of freeing up Deep Space Network (DSN) antenna resources. On the other hand, the level of future performance of the DSN ΔDOR group delay is expected to be similar to the performance level obtained from phase delays, due to a wider separation of tones at 32 GHz (Ka-band) with a reduction in the group-delay system noise error.

The frequencies used for the spacecraft tracking signals are near 2 and 8 GHz (S-band and X-band); however, the DSN is in the process of deploying Ka-band (32-GHz) tracking for the future. The 2005 Mars probe will be equipped with Ka- and X-band transponders. We expect that most future space probes will operate at Ka-band past this decade. This higher tracking frequency will provide increased spectrum allocation and greatly reduced ionospheric effects. Improvement of tropospheric calibration using water vapor radiometer (WVR) observations is also likely. These improvements will aid in both the group-delay and the phase-referencing techniques. If the VLBA is used for future space probe navigation, it must be upgraded to 32 GHz, and the results from critical sessions must be made available within 12 hours. In anticipation of the necessary Ka-band quasar reference frame, the VLBI group at the Jet Propulsion Laboratory (JPL) initiated an international collaboration on a K-Q band (24 and 43 GHz) VLBI source survey with the VLBA [3]. The VLBA spacecraft navigation investigation benefited substantially from the source survey collaboration.

The final MER trajectory is one of the best determined deep-space probe trajectories and was chosen, in this article, for evaluating the potential of the phase-referencing technique. We report on observations on January 19, 21, and 23, 2004, adjacent to DSN ΔDOR observations for comparison. In Section II, we estimate the formal accuracy ratio between DSN and VLBA measurements. The estimation is based on the inner working and external assumptions of a least-squares analysis of the delay observables. In Section III, we summarize the data acquisition at the VLBA with the National Radio Astronomy Observatory (NRAO) effort of obtaining the spacecraft images and delays. In Section IV, the JPL analysis of the VLBA-measured delays is outlined. A comparison of the VLBA phase referencing and DSN ΔDOR astrometric results is given in Section V. The article is concluded in Section VI. Finally, the Appendix summarizes the concerns obtained from other spacecraft observations.

II. Performance Estimates

In this section, we describe the assumptions related to the ODP-determined least-squares estimation of the differential angular coordinates between the spacecraft and a quasar. In parallel, we will also estimate the performance difference between the VLBA and DSN according to the primary effects of the least-squares estimation. Systematic modeling errors will fully affect the *prefit*[5] residuals; however, their effect will be distributed, often in a not well-known fashion, among the postfit residuals and the angular position. The formal errors provided by the least-squares estimation are erroneous in the presence of systematic modeling errors; systematic errors do not propagate in the same way as uncorrelated noise. All error estimates in this article will be *formal* error estimates.

In the full configuration, the VLBA network consists of 10 stations with 45 associated baselines, while the DSN ΔDOR utilizes 2 baselines at different epochs. However, the VLBA baseline observables are not independent since all stochastic errors are originated somewhat independently at each station. Therefore, the VLBA contains at most 9 independent baselines and the expected improvement of VLBA over the DSN, due to the increased number of baselines, is $\leq\sqrt{9/2} = 2.1$.

Declination is not well measured with ranging and Doppler techniques; therefore, the spacecraft-to-quasar angular measurements are frequently more decisive for declination than right ascension determination. This is due to the geometry of ranging, which is confined approximately to the ecliptic plane and involves the orbital motion of Earth. Unfortunately, due to the larger effective East–West than North–South geometric extension of both DSN and VLBA, the declination is not as well determined from quasar measurements as is the right ascension. The mean declination-to-right-ascension error ratio is approximately 2 for the DSN and 1.7 for the VLBA.

The DSN ΔDOR postfit scatter is approximately 40 picoseconds (ps) for the MER trajectory. This scatter corresponds to an angular performance[6] of $3 \times 10^{-7}(40/10,000) = 1.2$ nrad, which translates into about 1.3 and 2.6 nrad DSN errors for right ascension and declination, respectively. For the VLBA data, the estimated baseline-length dependence of the VLBA residual scatter, as discussed later in this section, will give 10-ps residual delay scatter, which is the value used by the final ODP estimate based on the residual delay scatter of iterated ODP estimates of spacecraft orbit. When one evaluates the VLBA performance of the collection of the variable baseline-length observations of the VLBA, the above delay scatter value of the VLBA is interpreted as a measure of delay scatter at the effective baseline-length of the VLBA. From the above delay scatter value, the angular performance of the VLBA is $3 \times 10^{-7}(10/3000) = 1$ nrad.[7]

A fundamental assumption in our analysis is that the ratio of the mean right-ascension error (per baseline) to the angular-performance value is nearly the same for the DSN as for the VLBA. The value of this ratio is not far from unity, because the declination of the sources is near zero ($\approx +10$ deg) and the VLBI observations are optimized such that the mean baseline is perpendicular to the source direction approximately at the mid-epoch of the observing session. In addition, the geometry of both the VLBA and DSN is dominated by the right-ascension-projected baseline coordinates.

When the delay-observable covariance matrix is diagonal with uniform delay error values, the least-squares estimation will consider all observations with equal weights. However, the geometry will be different for each scan and, in particular, there will be geometric differences between the groups of 45 baseline

[5] *Prefit* residuals refer to the observed minus the a priori model delays. On the other hand, *postfit* residuals are the observed delays minus the model delays obtained after correcting a group of a priori model parameter values, including the spacecraft trajectory position. The corrections are the result of a statistical estimate based on the observed delays.

[6] The *angular performance* is defined here as the mean of the baseline-length-divided root-mean-square of delay residuals belonging to each baseline. Therefore, the angular performance is a mean measure of angular error for a *single* baseline.

[7] From Fig. 4(b), which is based on the ODP postfit scatter, the angular performance is 1.4 nrad and is 1.1 nrad without 4 outliers.

observables. For further analytic estimates, we need to replace the lengths of the 45 baselines of the VLBA with a single effective baseline length. Assuming that the geometric differences average out among the 45 baselines, we make the simplest choice by assigning the mean value of VLBA baseline lengths of approximately 3000 km to the effective baseline length. Based on the simplest model of weighted least-squares estimation, it turns out that the mean baseline length is a correct choice. Considering the angular error σ_α of source position determination from 45 independent baselines that are approximately perpendicular to the source, we have that $\sigma_\alpha = (\sum_{i=1}^{45}(B_i/\sigma_i)^2)^{-1/2} =< \sigma > (\sum_{i=1}^{45}(B_i < \sigma_i > /\sigma_i)^2)^{-1/2} = (1/\sqrt{45})(< \sigma > / < B >)$, where $< B >= ((1/45)\sum_{i=1}^{45}(B_i < \sigma >)/\sigma_i)^2)^{1/2}$, with $< \sigma >$ as the root-mean-squared (rms) average of the baseline-delay scatter σ_i, and the baseline length B_i is given in delay units in these formulas. From the distribution of the assumed baseline-length-dependent σ_i discussed later in this section, we get that $< \sigma >= 10$ ps, and $< B >$ is approximately 3000 km.

In comparison, the two DSN baselines are nearly equally long with a mean of nearly 10,000 km. Consequently, the VLBA would have a $3000/10,000 = 0.3$ geometric performance loss if the delay errors were identical and baseline-independent. The effective delay errors, however, are lower for the VLBA due to its low phase-delay system noise in comparison with the DSN group-delay noise contributions. In addition, the VLBA errors are a complex combination of constant and baseline-dependent components. The contribution from Earth-orientation and ionospheric propagation delay uncertainties will be mostly proportional to the baseline length, while the tropospheric propagation delay uncertainties are largely independent of the baseline length on the longer baselines if the elevation angle is fixed. However, the elevation angles will need to be lower on the long baselines than on the short ones, giving another source of baseline dependence for the tropospheric delay error.

The VLBA MER errors were estimated using the DSN error estimates[8] as a guideline. In the chart of this DSN error estimate,[9] the errors were estimated for a 6-deg angular separation with adverse conditions for geometry, media delays, and instrumental effects. The separation angle between the MER spacecraft and reference quasar is about 2.5 deg for our data. After scaling the errors appropriately by factors of 2 to 3, it is estimated that the mean VLBA MER delay error consists of about a 7-ps constant contribution and a baseline proportional component with a value of 20 ps at the 10,000-km baseline length.[10] The two components are assumed to be root-squared-summed (rss) with an rms mean value of $< \sigma >= 10$ ps. Therefore, the VLBA is expected to have a lower MER formal angular error than the DSN with an angular performance of $3 \times 10^{-7}(10/3000) = 1$ nrad and a VLBA-to-DSN performance gain ratio g of

$$g \leq (40/10)(3,000/10,000)\sqrt{9/2} = 2.5 \tag{1}$$

The improvement factor of Eq. (1) may be less than 2.5, since the correlation among the different-station delay observables reduces the number of independent stations from 9 to a currently unknown value. Note that Eq. (1) does not include some detailed effects of least-squares estimation, e.g., the influence of the a priori position error of the quasar.

Due to the difference in geometry, the corrected DSN-to-VLBA declination error ratio g will be $(2/1.7)2.5 = 2.9$. With this result in hand, we are able to estimate the VLBA-determined declination error from the corresponding DSN error of 2.6 nrad as $2.6/2.9 \approx 0.9$ nrad. Including the effect of the assumed 0.7-nrad error for the a priori quasar position on the least-squares estimates, we have the

[8] J. S. Border, "2004 Error Budget for DSN Delta Differential One-way Range Measurements," JPL Interoffice Memorandum 335-04-04-D (internal document), Jet Propulsion Laboratory, Pasadena, California, July 9, 2004.

[9] Ibid.

[10] The error estimate should be refined; there currently are too many interpretive possibilities between a few and a 20-ps scatter. Also, compare these values with the estimates of 6-ps constant and 17-ps linear (at 10,000 km) terms obtained in Section V from Fig. 4(a), which describes the baseline dependence of the VLBA postfit scatter. However, the latter values were obtained from a group of very limited samples of atmospheric conditions: three 4-hour sessions within 4 days.

effective VLBA-determined declination error as $\sqrt{0.7^2 + 0.9^2} = 1.1$ nrad. Therefore, the performance ratio, as it would be obtained from a least-squares estimate, becomes approximately $2.6/1.1 = 2.4$. As is seen in Section V, the presented ODP estimate of the declination formal error is 1.2 nrad, and the VLBA–DSN formal accuracy ratio is $2.4/1.2 = 2.0$.

One could argue that the VLBA performance is actually dominated by its longest baselines. However, this does not appear to be the present case, because the large number of shorter baselines with a smaller delay error is equally important in the above consideration; we will demonstrate this effect below. If the delay errors were strictly linear with the baseline length, without a constant component, then the angular performance of all baselines would be the same. Because of the presence of the constant delay error behavior at the short baseline range, here the angular error will be larger for a *single* baseline.

Thus, let us use the delay observables of only the two longest independent baselines with a reasonable geometry for a statistical estimation, MK–HN and BR–SC.[11] According to the estimate above, at 6500 km the delay scatter is 15 ps, while the rms mean value is 10 ps. Therefore, the angular error at the mean baseline length will be higher at the 3000-km length by a factor of $(10/15)(6500/3000) = 1.4$. Let us now take 9 independent baselines with the mean value of 3000 km. This will give us a factor of $\sqrt{9}$ improvement for the 3000-km case, while only a $\sqrt{2}$ for the two long baselines. Thus, the ratio becomes $\sqrt{(2/9)}(10/15)(6500/3000) \approx 0.7$, which shows that the sum of all baselines performs somewhat better than the two long ones. The conclusion is that the astrometric strength of the VLBA is not necessarily associated only with its longest baselines.

III. Data Acquisition and Image Processing: The NRAO Effort

The phase-referencing technique alternates observations between one or more quasars and the spacecraft. Each scan is a 40-second integration on the quasars and spacecraft, with about 20 seconds of slew and setup time between sources. The approximate observing frequency is 8.4 GHz. Several quasar/spacecraft cycling schemes have been investigated over the many sessions. The critical inputs for the spacecraft observations are the frequency range of the telemetry signal, its polarization, and the spacecraft orbit. Agreements between JPL and NRAO during the last year increased the efficiency of transferring these needed inputs for the observation and correlation of the VLBA data.

Both the quasar and spacecraft were observed with 2-bit sampling over a 16-MHz bandwidth, separated into 256 channels with 62.5-kHz width. The signal-to-noise ratio (SNR) for the quasar over a 16-MHz bandwidth, and for the spacecraft over a 62.5-kHz bandwidth, was >50 over a 40-s scan, producing errors already smaller than those associated with the variable troposphere refraction over each antenna. The spatial coherence properties from the non-coherent radiation of a quasar and from the telemetry signal of a spacecraft are identical, unless the spacecraft signal is extended in angle and has a modulated phase difference as a function of angle. Thus, the delay information obtained from cross-correlation for the coherent narrowband signal of a spacecraft should be identical to those of a non-coherent radio source, though the statistical properties of the correlation error are different for a random noise signal than for a deterministic pulse. The VLBA experiment parameters for each scan with the main International Celestial Reference Frame (ICRF) calibrator source are given in Table 1.

The reduction and calibration of the data were similar to those used in reduction of normal phase-referencing observations. First, the a priori calibrations were applied to the data; this included the use of a Goddard Space Flight Center (GSFC) CALC astrometric/geodetic model in the correlator. Second, a high-quality ICRF quasar was used as the phase reference. Because of a precise a priori model, the variations of the antenna-based quasar phases were small and could be easily connected between subsequent quasar observations, several minutes apart. The phase variation was at the level of

[11] BR = Brewster, Washington; HN = Hancock, New Hampshire; MK = Mauna Kea, Hawaii; and SC = Saint Croix, Virgin Islands.

Table 1. Configuration parameters.

Source	Rate, Mb/s	Band-width, MHz	Sample bit	Frequency, MHz	Name	Duration, s	Separation, s	Difference angle, deg	Elevation angle, deg	SNR
Quasar	64	16	2	8434.89	J0121+1149	40	480	2.5	>30	>50
Space-craft	64	256 × 0.0625	2	8434.89	MER-B	40	120	0	>30	>100

∼30 deg = 10 ps for the 1-minute duration, and it was larger at the low elevation angles (∼30 deg) and in bad weather conditions. Because the spacecraft and quasar were observed over a different frequency range, we used a strong calibrator source (3C454.3) in order to determine the non-linear phase versus frequency characteristics of each telescope. These are stable for many days, and we estimate a possible frequency-dependent phase difference between the quasar and spacecraft to be less than 3 deg, about 1 ps.

Next, the interpolated quasar phases were applied to the spacecraft. Finally, the position of the spacecraft was obtained by Fourier imaging of the calibrated data, with subsequent deconvolution. The image quality with more than 5 minutes of data is not signal-to-noise limited, but is degraded by residual tropospheric phase errors between the quasar and the spacecraft. These errors can be reduced using multiple calibrations. The peak-to-highest-side-lobe spacecraft image intensity is generally >5:1 with a relative *internal* positional error of <0.1 mas, while a more realistic estimate of the relative image-center error yielded about 0.2 mas (1 nrad). Note the importance of proper media-delay calibration; uncalibrated media delays can result in a distorted image with an ambiguous and/or erroneous image center.

The spacecraft position with respect to the quasar can be obtained in two ways. First, the location of the peak of the image after the above calibration gives the offset between the true position of the spacecraft and that assumed by the orbit model and other calculations used in the correlator. Thus, this center of image position is critically tied to the correlator model, which phenomenon will be absent in the second approach of total-delay-based reduction.

The correlation of the first few spacecraft experiments revealed a fault in the correlator model, which displaced the derived images by up to 5 mas from the expected previously determined spacecraft ephemeris positions. This was traced, eventually, to the use of an approximation in the GSFC CALC software, which treats all radio sources as being outside the solar system in computing gravitational bending. The occurrence of this fault emphasizes the model-dependence of this approach.

The imaging results for the three VLBA sessions are shown in Fig. 1, and they suggest two major points. First, using the position of the ICRF source J0121+1149 as the reference, the apparent average offset of MER-B over the 4-day period was 0.16 mas (0.8 nrad) west and 0.5 mas (2.5 nrad) south of the assumed position used in the correlator. Hence, the deviation of the spacecraft is nearly $2\,\sigma$, which marginally suggests that the average spacecraft offset is non-zero. Secondly, the spacecraft shows a motion from north to south with respect to all calibrators. Since these calibrators surround the spacecraft, the drift is unlikely to be caused by differential tropospheric effects that would produce a different drift among the sources. The change over the 4-day period is 0.6 mas (3 nrad), to the south. This apparent motion is independent of the a priori position error of the source and only depends on the daily errors; hence, the significance of the 0.6-mas shift is at the level of $(3/1)/\sqrt{2/3} = 3.7\,\sigma$, assuming a 1-nrad error per data point and three pairs of independent measurements of the drift.

An ODP analysis of the VLBA observations independently for each day is needed to determine the validity of the spacecraft offset and its apparent drift as seen in the imaging result. As an alternative, one

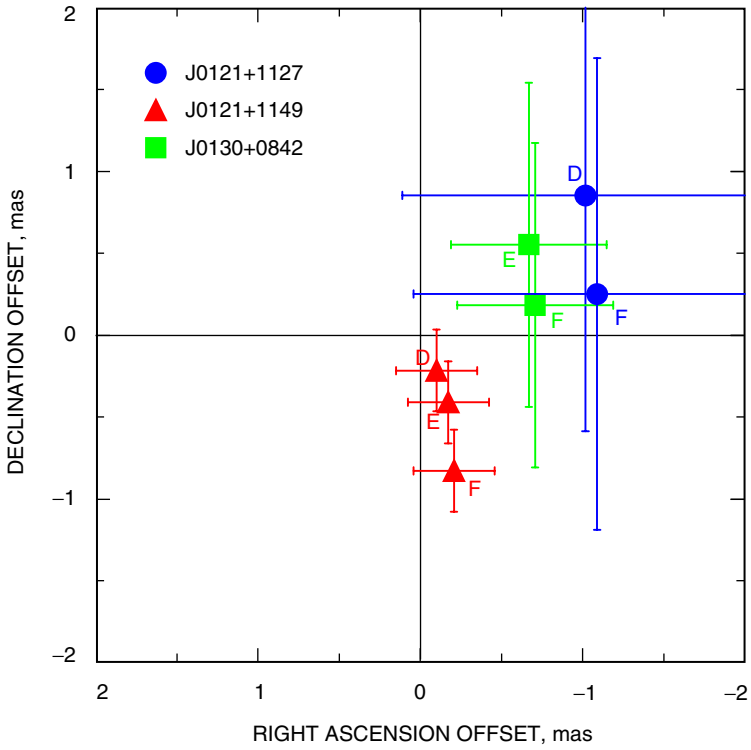

Fig. 1. The ephemeris position of the spacecraft relative to the three different quasars. Each quasar is shown by the indicated color, and the letter code gives the observing session: D = January 19, E = January 21, and F = January 23. The estimated position errors of the three quasars, shown by the error bars, include the a priori uncertainty in the position plus an estimated accuracy for each day's observations.

needs to estimate the ephemeris error of the differential spacecraft position between January 19 and 23. If the image-center drift is in conflict with the spacecraft ephemeris knowledge, then the VLBA spacecraft-related models need further investigation. The process of obtaining an image center is relatively simple; however, the measured position offset of the spacecraft is tied to the accuracy of the correlator model, which cannot be properly corrected in the final analysis by the ODP.

The second way of determining the spacecraft relative position is to use the observed total delays of the spacecraft with respect to that of the quasar by a least-squares estimation method. The quasar total delays were determined from the model applied in the correlator (geometric delay, clock delay, and tropospheric delay), using an Astronomical Image Processing Software (AIPS) module based on that used by the GSFC VLBI group to input delays into their CALC-SOLVE estimation program that is equivalent to the JPL MODEST software. The model ionospheric delay was calculated at a later step in the AIPS reduction. A clock-like residual-delay term that is identical for both the spacecraft and the quasar was not added back to the total delay. The magnitude of this delay term is rarely more than 300 ps, and the omission of this term results in a <2-ps error.

The spacecraft total delays were determined from correlator model terms similar to those for the quasar, plus two additional contributions: the delay associated with the approximate spacecraft position offset as found by imaging, plus any residual baseline phase, converted into delay. These total delays should be independent of the correlator model, and this is demonstrated in Fig. 2, which shows the total delay differences for the quasars (0.3-ps rms) and for the spacecraft (0.8-ps rms) using two different correlator models for the January 23, 2004, data sets. The spacecraft orbit differs by about 30 mas

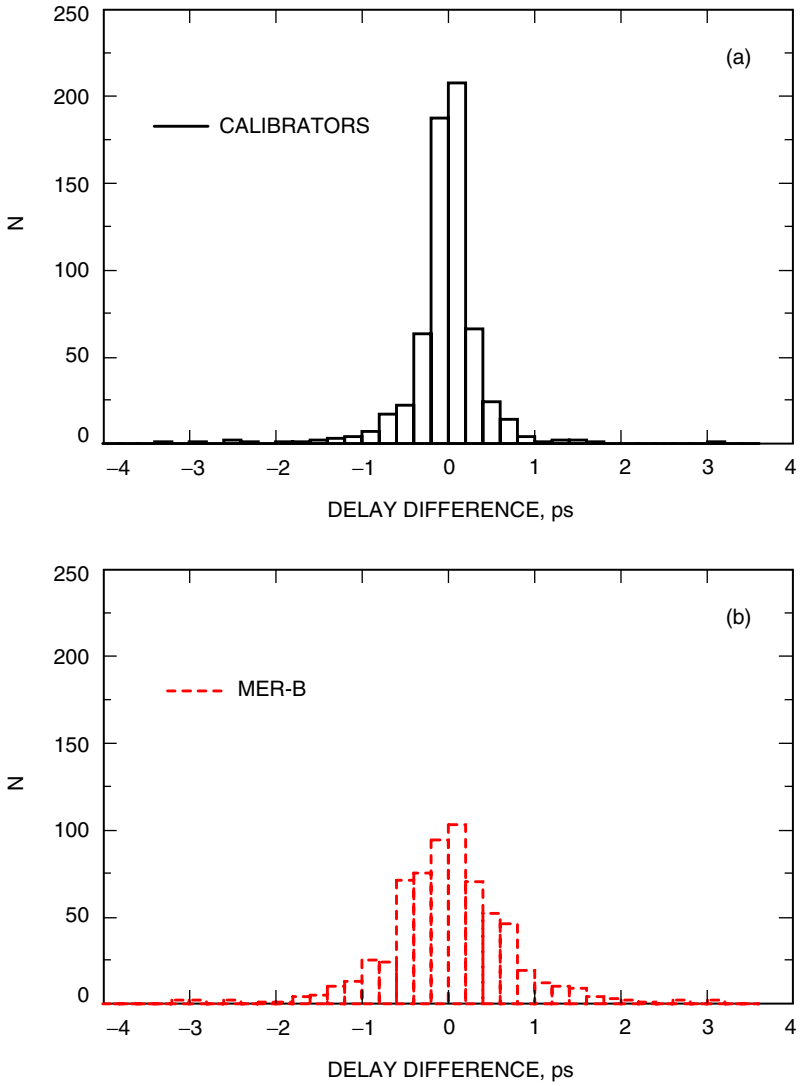

Fig. 2. Distribution of total delay differences from two correlation passes of the January 23, 2004, experiment for (a) the three quasars and (b) the spacecraft. The rms scatter is 0.3 ps for the quasars and 0.8 ps for the spacecraft. The two correlator models of the spacecraft orbit differ by 30 mas.

(150 nrad) between the two correlation passes. The rms scatter of 0.3 ps is typical for two correlation passes with no changes in the correlation model that would affect the quasars. The spacecraft delay scatter is 0.8 ps, somewhat larger than for the quasars, but at a level of 0.1 nrad (0.02 mas) in effective position error. It must be emphasized that the imaging is an essential part of the reduction and a crucial part of obtaining the total delays. Imaging effectively resolves all the cycle ambiguities in the individual baseline phase measurements and provides the VLBA's observational result for incorporation in a model-independent interface to further JPL analysis.

The quasar and spacecraft delays, with other information about the a priori calibrations, were written in an ASCII format for delivery for the subsequent JPL analysis.[12]

[12] E. Fomalont, "The Processing of VLBA Spacecraft Data," NRAO Memorandum, National Radio Astronomy Observatory, Charlottesville, Virginia, January 3, 2005.

IV. Delay Observable Processing: The JPL Effort

In VLBI measurements, the radio signals arriving from the same source are recorded at multiple stations with approximately synchronized time tags at each station. The VLBI delays are the difference in station clocks of signal arrivals at any of the station pairs. The ΔDOR data input of the ODP consists of differential one-way ranges for spacecraft and single-station time-referenced VLBI delays for the quasars. The differential one-way range of a spacecraft is the difference in spacecraft-to-station range delays, which are based on the time tags when the wave front impinges at each telescope.

The additional AIPS routine described in Section III provides the above conventional VLBI delays for both the quasar and the spacecraft. Therefore, the spacecraft delays were converted into one-way range delays with a modified ΔDOR interface program.[13] In addition, the necessary interface and procedures were developed to handle a complete experiment and analyze performance issues and the quality of the data before the delivery to navigation.[14] The obtained delivery route to navigation of the pre-processed VLBA data is similar to that needed to include DSN ΔDOR observations.

It should be emphasized again that the data input to the ODP are *total* delays that are based on the actual arrival times of the signals. Therefore, the ODP measures of delays can be evaluated nearly[15] independently of the models used in the original measurements. That is the reason we sought to restore the phase-referenced phases to total delays in the first place. Based upon these principles and the experience with the data analysis, it was decided that the restored total phase-reference delays would be the VLBA-tracking-to-navigation interface for the immediate future.

The use of total delays enables an analysis with any model of observables. In the current data reduction, there were no attempts to replace the correlator–AIPS-used estimates of tropospheric and ionospheric delays[16] with better external calibrations, except that the ODP estimated and applied additional total (dry + wet) tropospheric zenith delay estimates for each observing session. These corrections amounted mostly to a few millimeters—in the extreme case to 20 mm. The overall effect of these corrections to the spacecraft position was nearly negligible. There was also a necessary VLBA station location change from the ITRF 2000 frame used by the astrometric community to the self-consistent 1993 epoch, and the ODP applied a somewhat revised version of Earth-orientation parameters used by the VLBA.[17]

It is frequently emphasized throughout this article that the spacecraft-to-quasar navigation is limited by the positional accuracy of the quasar. However, determining the true positional accuracy of a quasar at a given epoch is nearly impossible. What we have is rather a lower and upper bound on the positional accuracy. The ICRF catalog [4] of quasars has almost a uniform accuracy of 0.25 mas (1.25 nrad) because it cautiously inflates the errors such that the catalog will have guaranteed error values at future epochs. However, formal errors from the least-squares estimation based on two decades of observations can be more than 10 times lower. Thus, the real error lies between these low formal values and the inflated error values. For the ICRF quasar J0121+1149, the MODEST-based estimate of 0.7 nrad was chosen for the ODP analysis in this article.

---

[13] J. S. Border, "A Model for VLBA Spacecraft Delay Observables," JPL Interoffice Memorandum 335-04-01-D (internal document), Jet Propulsion Laboratory, Pasadena, California, March 11, 2004.

[14] G. Lanyi, "Initial Assessment of the VLBA S/C-Quasar Differential Angular Measurement," JPL Engineering Memorandum 335-04-03-D, Jet Propulsion Laboratory, Pasadena, California, June 4, 2004.

[15] There are some small secondary modeling error effects due to the combination of the correlator and AIPS processing which are not easily remodelable.

[16] Normally, *positive* ionospheric group *delays* are subtracted from group delays, but are added to phase delays for calibration. In our case, the positive GPS-based ionospheric delay values supplied with the phase-delay values needed to be *subtracted* from the phase delays for appropriate calibration. This sign issue remains to be fully resolved.

[17] T. J. Martin-Mur, "Navigation Analysis of the MER-B VLBA Data," JPL Presentation (internal document), Jet Propulsion Laboratory, Pasadena, California, September 24, 2004.

The analysis is done in two steps. First, the delay residuals of the VLBA data, including their media calibration, are evaluated using the known a priori values of all model parameters; this results in the *prefit* residuals. The a priori model parameter values include the ICRF quasar position, the station coordinates, the Earth-orientation parameters, and, beside other parameters, the spacecraft positions from an ephemeris, which are based on DSN ranging, Doppler, and DSN ΔDOR differential angular measurements during the entire mission.

The second step *should* consist of

(1) Determining the weight matrix that is the inverse of the covariance matrix of delay observables. The effect of a partial implementation of this step is mitigated if item (3) involves an estimate of the relevant stochastic processes (e.g., by Kalman filtering). However, neither an external calibration nor a statistical estimate will fully remove stochastic contributions to observables.

(2) Constructing the a priori covariance matrix of observable parameters, e.g., source position, etc.

(3) The actual statistical least-squares estimation of the spacecraft orbit and other secondary parameters based on the prefit residuals.

(4) An analysis of the obtained *postfit* residuals.

(5) An analysis of the new spacecraft position and its error.

For the second step, first the overlapping 9 sessions (on 5 sequential days starting with January 19) of DSN range, Doppler, and ΔDOR prefit residuals based on the final MER-B DSN solution were included with the 3 sessions of VLBA prefit residuals using identical a priori parameter values.

Then came the difficult task of item (1). It is fair to say that no existing least-squares-fit software will do this task in a fully appropriate fashion for all observables involved in the observed data. For this task, one needs an estimate of the error of the delay observable for each scan of all baselines, and the correlation between all pairs of these delay observables. In the absence of a well established error covariance estimate, one needs to have a few external adjustments.

First of all, we set all off-diagonal correlations to zero. This will be compensated by an appropriate adjustment of the diagonal elements. The delay errors can be estimated in an iterative fashion by sequential estimates. Since there is no correlation assumed between data points, the diagonal elements then must be appropriately weighted. The DSN ΔDOR delay error was used as the base with its measured postfit 40-ps scatter. The DSN spacecraft-range and the two-way Doppler-shift results then were matched against the ΔDOR and set to 14.1 range units[18] and 4.2 mHz, respectively.

For the VLBA angular measurements, a delay scatter of 10 ps was chosen, which lies between the prefit 12.9-ps and postfit 9-ps values. However, the VLBA and DSN ΔDOR data must be matched to obtain a reasonable comparison by either ignoring part of the VLBA data or de-weighting it. There were approximately 12 times more delay observables in the VLBA than in the DSN ΔDOR data, and thus the VLBA delay error was inflated by a factor of $\sqrt{12}$. If one were interested in absolute VLBA performance by using only the VLBA data in a least-squares fit for quasar position determination, then one would also have to enlarge the delay error, since all near scans are correlated on a baseline. If about 1 hour is considered to be sufficient for de-correlation between scans, then one would use an inflation factor of $\sqrt{8}$, since the ICRF quasar observations are 8 minutes apart, giving only a 20 percent smaller delay error than the above 10-ps residual delay scatter.

[18] 1 MER range unit is approximately 30 cm.

In addition, as discussed in Section III, the VLBA delay data need further de-weighting due to the correlations among the 45 baselines. Since there are fewer than 9 statistically independent baselines, the de-weighting is accomplished by inflating the VLBA delay error by an additional factor of $\sqrt{45/9}$; thus, the correlations among different-station delay observables were ignored. This factor is also applicable for the case when only VLBA delay data are used in a least-squares estimation. For item (2), the a priori parameter correlation matrix is assumed to be diagonal in general, and the angular uncertainty of the quasar is assumed to be uniformly 0.7 nrad, as previously discussed. The station-location coordinates were constrained to a 3-mm uncertainty level. The results of the analysis under items (3), (4), and (5) will be discussed in Section V.

V. Comparison of VLBA and DSN Results

All sessions of the VLBA and DSN observations included the quasar J0121+1149 (P 0119+11) as the primary reference. It is a high-quality ICRF radio source with little structure and with an estimated position error of 0.15 mas (0.7 nrad) in both right ascension and declination. This positional error is relative to the ICRF frame itself, and the ICRF frame is tied to the planetary frame with a larger error. Therefore, the total differential angular error between the quasar and the spacecraft is at least 0.7 nrad. However, both DSN and VLBA measurements utilize the same quasar; thus, a differential angular offset between DSN- and VLBA-based angular measurements is due to other sources of error.

The differenced delay residuals between the spacecraft and the quasar referenced to a priori models, including the previously determined spacecraft ephemeris, will confine the magnitude of the differential angular position error. This residual delay is a time-varying function for each baseline. Receiver noise and residual clock errors will tend to produce random noise, but any spacecraft offset and atmospheric residual errors will cause a systematic effect. In Fig. 3(a), we show the average absolute values of the residual delay error for the VLBA observations, each of 4-hour duration, for each baseline as a function of baseline length for all 3 days. These points show a rough linear slope with baseline length, an indication of an angular offset with a magnitude at the level of 1 nrad. The baseline-rms-averaged residuals then are divided by their baseline length, resulting in a distribution of an angular-error measure with a mean value of 1.9 nrad of *angular performance* ($\sim$1/10 fringe spacing), which is shown in Fig. 3(b).

Some component of these residuals may be caused by an offset from the assumed spacecraft ephemeris position. For example, an offset of 1 nrad (in the order of the MER orbit uncertainty) would produce a delay residual at a 10,000-km baseline length up to 40 ps. In Fig. 4(a), we show the average absolute values of the residuals for the VLBA observations as a function of baseline length, *after statistically estimating and removing the offset.* The remaining delay residuals are probably dominated by atmospheric refraction differences between the spacecraft and quasar. Figure 4(b) shows the distribution of the corresponding absolute angular errors. The mean value is 1.4 nrad. If the four largest outliers are removed, the mean value is 1.1 nrad.

The conclusions from Fig. 4(a) suggest that, for the VLBA, phase-referencing residual delays have a floor rms of 6 ps and a linear term that is 17 ps at 10,000 km. For comparison, the DSN ΔDOR post-fit residual scatter is approximately 40 ps for a baseline of 10,000 km. Thus, the 10,000-km projected VLBA delay scatter implies slightly more than a factor of two improved angular sensitivity on two statistically independent long VLBA baselines that are geometrically equivalent to the DSN. In general, however, one cannot directly interpret this number without the detailed considerations of Section II with the number of independent baselines, the baseline-length dependence of the residual delay scatter, and the a priori quasar position error.

Figure 5 shows the estimated spacecraft trajectory intersections on the Mars B-plane [5] and the corresponding 3-σ error ellipses for the DSN and DSN-plus-VLBA solutions. The addition of the VLBA data moved the declination-oriented ($\approx$N–S) coordinate by -1.6 nrad within 1 σ of the purely DSN-determined 2.4-nrad error value. Note also that the B-plane 1-σ declination-oriented error of 1.2 nrad

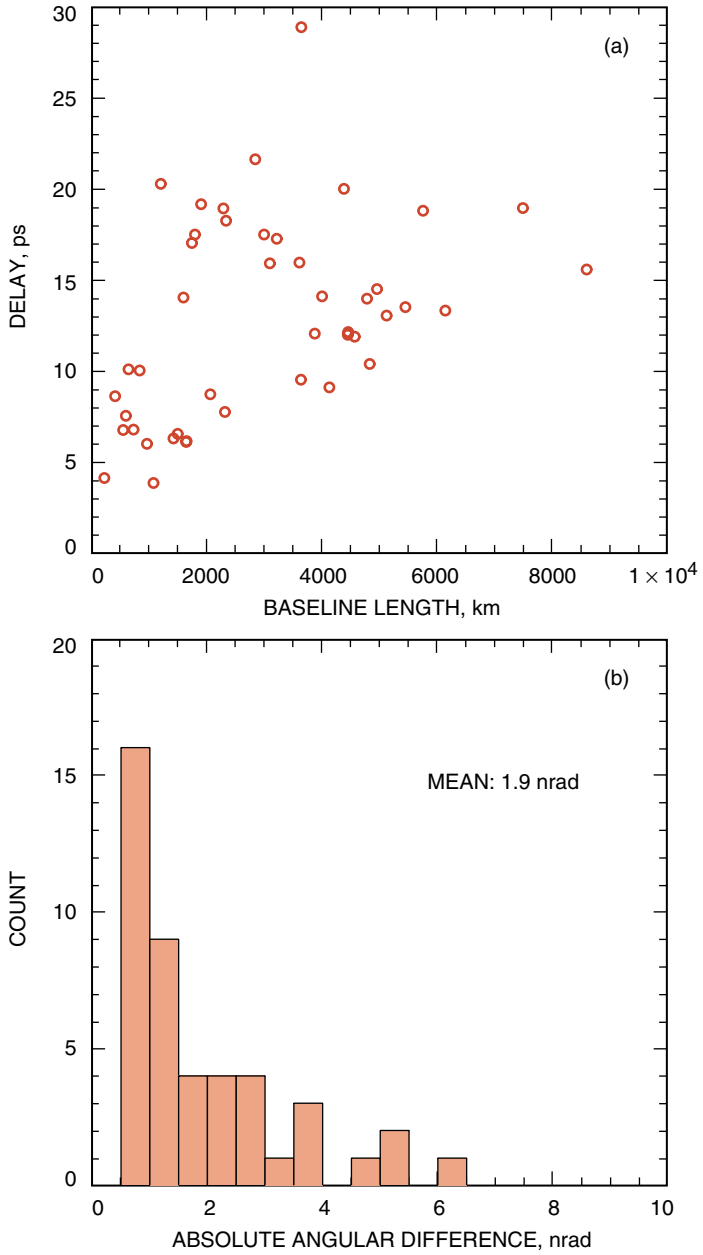

Fig. 3. Graphs of prefit residual rms per baseline: (a) prefit absolute differential residual delays as a function of the baseline length and (b) distribution of the corresponding prefit absolute angular differences.

is on the order of the image-center accuracy estimate of 1 nrad. The right ascension (E–W)-oriented component is not appropriate for VLBA *performance* comparison since its errors appear to be dominated by spacecraft ranging data and a priori source position errors. The spacecraft coordinate offsets relative to the spacecraft ephemerides are in the same right ascension–declination quadrant for the mean value of VLBA image centers corresponding to J0121+1149 (Fig. 1: +0.8 and −2.5 nrad) and for the ODP B-plane estimate (+0.3 and −1.6 nrad, right ascension and declination).

As we discussed at the beginning of Section II, the presence of systematic errors can distort the formal error estimate given by a least-squares estimation. Thus, one needs to pay careful attention to possible

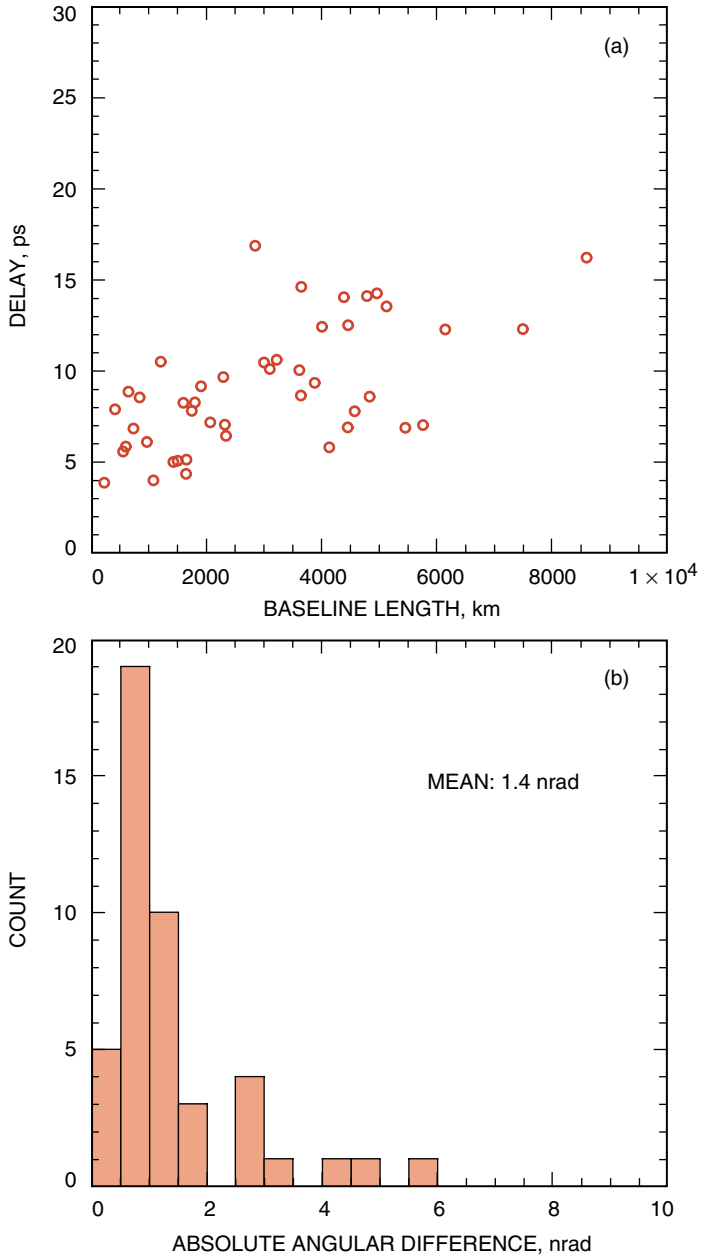

Fig. 4. Graphs of postfit residual rms per baseline: (a) postfit absolute differential residual delays as a function of the baseline length and (b) distribution of the corresponding postfit absolute angular differences.

systematic errors. For example, the error ellipses in Fig. 5 do not include the effect of an error in the Mars ephemeris or the effect of a systematic offset between the target body and the ICRF quasar source.

VI. Conclusion

The VLBA-based phase-referencing technique performed well on the MER trajectory and provided angular spacecraft coordinates quite within the statistical uncertainty of the predetermined trajectory. The ODP-based estimate of formal error of the *declination*-determined B-plane coordinate component is 1.2 nrad for the VLBA, which is smaller than the corresponding current DSN MER error of 2.4 nrad; this

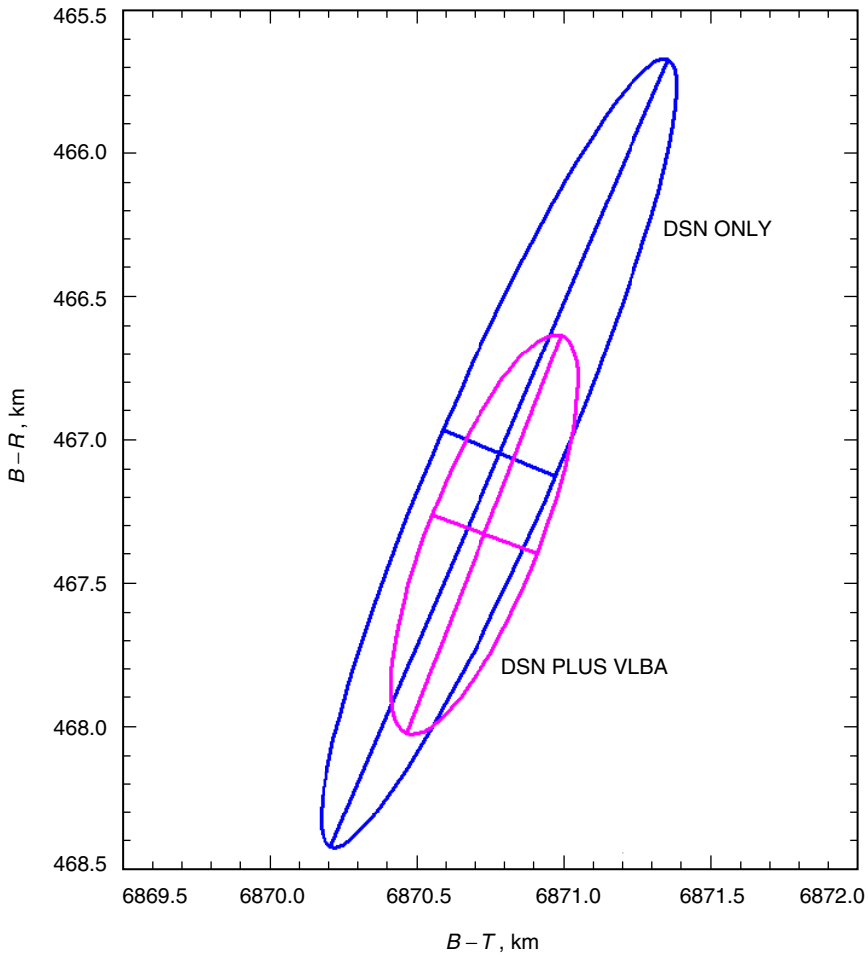

Fig. 5. B-plane projected spacecraft position with 3σ error ellipses. The grid spacing is 0.1 km (0.5 nrad). The outer ellipse represents the DSN standard solution. The VLBA data are included in the inner ellipse solution. The major axis of ellipses corresponds approximately to the declination direction of the spacecraft.

factor of two largely agrees with the given analytic estimate. It should be noted that the comparison is already limited by the uncertainty of the a priori quasar position. Hence, the improvement of the ICRF catalog, especially at 32 GHz, should have high priority.

Note again that in actual ODP trajectory error estimates the VLBA precision improvement would be mitigated by the larger errors of the Mars ephemeris position and the planetary-to-inertial-frame tie. These errors are ignored in the ODP estimates presented in this article in order to exhibit the internal precision of the VLBA measurements.

Also, for phase referencing to succeed, it is necessary to observe a quasar with well-known coordinates that is within 4 deg of the spacecraft. The current ICRF catalog is not dense enough to fully support astrometric phase referencing on a spacecraft trajectory; therefore, additional radio source catalog development will be needed.

The VLBA offers a precision advantage for measurements made today at X-band. Certain navigation problems that need ultimate precision to diagnose potential systematic errors that are otherwise undetectable could benefit from the VLBA measurements. As spacecraft communication frequencies migrate

from X-band to Ka-band, and larger bandwidths are available for group delay measurements, the precision difference between DSN ΔDOR and VLBA phase referencing will be mitigated.

Finally, the VLBA with 10 telescopes and 45 baselines has built-in redundancy for the reliability of results. The large number of baselines facilitates the determination of unambiguous differential spacecraft positions, even in the presence of relatively large phase scatter. Furthermore, it is simple to recognize and remove whatever, if any, antenna data are below the performance standard, either because of instrumental problems or atmospheric turbulence. In addition, the non-invasive nature of VLBA observations without the use of dedicated spacecraft tones is an advantage under specific circumstances.

Acknowledgments

We express our appreciation for the advocacy of the described navigation technique and for the continuous encouragement and support from Barry Geldzahler and Jim Ulvestad. We also thank Charles Naudet for his relentless team organization efforts and technical comments.

References

[1] C. L. Thornton and J. S. Border, *Radiometric Tracking Techniques for Deep Space Navigation*, JPL Deep Space Communications and Navigation Series, J. H. Yuen, ed., New Jersey: John Wiley & Sons, Inc., 2003.

[2] J-F. Lestrade, A. E. Rogers, A. E. E. Whitney, A. R. Niell, R. B. Phillips, and R. A. Preston, "Phase-Referenced VLBI Observations of Weak Radio Sources. Milliarcsecond Position of Algol," *Astronomical Journal*, vol. 99, pp. 1663–1673, 1990.

[3] C. S. Jacobs, P. Charlot, D. Gordon, G. E. Lanyi, C. Ma, C. J. Naudet, O. J. Sovers, L. D. Zhang, and the K-Q VLBI Survey Collaboration, "Extending the ICRF to Higher Radio Frequencies: Initial Global Astrometric Results," AAS meeting, Seattle, Washington, January 8, 2003, *Bulletin of the AAS*, vol. 34, no. 4, session 76.10,
`http://www.aas.org/publications/baas/v34n4/aas201/1241.htm`

[4] C. Ma, E. F. Arias, T .M. Eubanks, A. L. Fey, A. M. Gontier, C. S. Jacobs, O. J. Sovers, B. A. Archinal, and P. Charlot, "The International Celestial Reference Frame Based on VLBI Observations of Extragalactic Radio Sources", *Astronomical Journal*, vol. 116, p. 516, 1998.

[5] T. P. McElrath, M. M. Watkins, B. M. Portock, E. J. Graat, D. T. Baird, G. G. Wawrzyniak, J. R. Guinn, P. G. Antreasian, A. A. Attiyah, R. C. Baalke, and W. L. Taber, "Mars Exploration Rovers Orbit Determination Filter Strategy," AIAA-2004-4982, Providence, Rhode, Island, August 16–19, 2004.

Appendix
Observations and Recommendations

Based on the analysis of other spacecraft observations, six VLBA phase referencings,[19,20] and previous ΔDOR observations, the following comments may be useful.

(1) The measured total delays are insensitive to the accuracy of the input orbit, and offsets as large as 100 mas are routinely handled.

(2) The spacecraft signal is strong, often having higher SNR than the quasars. Any signal that is used for spacecraft telemetry clearly will be sufficiently strong for VLBA interferometry. The data are atmosphere-limited after only a few minutes of integration at X-band.

(3) Observations south of −10 deg will have larger errors, especially in the north–south direction, as shown by a Stardust spacecraft observation that is available. However, apart from the increased error, no additional problems were encountered.

(4) The quality of the results depends on the proximity of the quasar to the spacecraft. However, even near the galactic plane, it is rare not to have a quasar within 5 deg of the target. As described above, Very Large Array (VLA)/VLBA search observations can be made at least 1 month before the spacecraft observations to find additional quasars or to determine a quasar position within 0.5 mas of the ICRF frame. With the Mark-5 system, we expect to have significant increased sensitivity so that quasars can be found sufficiently close to a target to reduce this possibility.

(5) The MER-B VLBA experiments were 4 hours in length. We expect that 30-minute observations, especially at the highest elevation angles available, will provide more than sufficient accuracy, and these tests are continuing.

(6) The absolute accuracy of the VLBA-based spacecraft-position determination should be tested by making a series of measurements of spacecraft that are better tied to the ephemeris of Mars or another well-known body in the solar system other than the MER probe.

(7) Data reduction based on a less accurate a priori spacecraft ephemeris should be investigated.

(8) Investigate data reduction with large and unpredicted variation in spacecraft transmitter frequency.

(9) At the new DSN tracking frequency of 32 GHz, the phase errors will be a factor of 4 larger than those at 8 GHz. This will make phase referencing somewhat more difficult since phase ambiguities will be more likely. However, the availability of a simultaneous dual-frequency capability (8/32 GHz, X-/Ka-band) at the VLBA would improve the accuracy by removal of the ionosphere refraction and aid the phase connection. A study, based on a 24-h S-/X-/Ka-band VLBI VLBA session, conducted for resolving this issue, indicated that sequential X-/Ka-X-band scans will calibrate only half of the Ka-band ionospheric delays.[21]

---

[19] E. Fomalont, "Analysis of the Cassini October 2004 Experiments," NRAO Memorandum, National Radio Astronomy Observatory, Charlottesville, Virginia, January 5, 2005.

[20] E. Fomalont, "Recommendations for the VLBA Observations of Spacecraft at 32 GHz," NRAO Memorandum, National Radio Astronomy Observatory, Charlottesville, Virginia, January 5, 2005.

[21] G. Lanyi, communication at a K-Q VLBI Source Survey Collaboration meeting, Washington, D.C., June 11, 2004.